29 Jan 90 Interim - March 89 - Jan 90

BALLISTIC RANGE FLOWFIELD MEASUREMENTS OF THE HYPERVELOCITY NEAR WAKE OF GENERIC SHAPES & CORRELATION WITH CFD SIMULATIONS.

WU - 25670323

G. BUTLER, D. KING, B. NGUYEN & G. ABATE, AFATL/FXA,
AFATL Program Manager

GENERAL DYNAMICS
CONVAIR DIVISION
SAN DIEGO CA

AFATL/FXA
EGLIN AFB FL

Aeromechanical Division
Air Force Armament Laboratory
Eglin Air Force Base, FL 32542

AFATL-TR-90-03

THIS PAPER DESCRIBES ANALYTICAL AND EXPERIMENTAL RESEARCH INTO THE STRUCTURE AND PROPERTIES OF THE NEAR WAKE OF GENERIC SHAPES AT SUPERSONIC FLIGHT CONDITIONS. THREE AXISYMMETRIC MODEL CONFIGURATIONS WERE CONSTRUCTED AND TESTED IN THE AEROBALLISTIC RESEARCH FACILITY AT EGLIN AIR FORCE BASE, FLORIDA AT MACH NUMBERS FROM 3 TO 5. LASER INTERFEROGRAMS WERE TAKEN OF THE NEAR WAKE OF THE CONFIGURATIONS AT SEA LEVEL CONDITIONS. COMPUTATIONAL INTERFEROGRAMS WERE THEN DEVELOPED AT IDENTICAL CONDITIONS AND WERE CORRELATED AGAINST THE EXPERIMENTAL DATA. THIS CORRELATION WILL HELP CALIBRATE HIGH SPEED CFD CODES IN THIS COMPLEX FLOW REGION.

NEAR WAKE
RECIRCULATION ZONE
INTERFEROGRAM
CFD CORRELATION

AEROBALLISTICS

8

UNC UNC UNC UL

GENERAL INSTRUCTIONS FOR COMPLETING SF 298

The Report Documentation Page (RDP) is used in announcing and cataloging reports. It is important that this information be consistent with the rest of the report, particularly the cover and title page. Instructions for filling in each block of the form follow. It is important to **stay within the lines to meet optical scanning requirements.**

Block 1. Agency Use Only (Leave Blank)

Block 2. Report Date. Full publication date including day, month, and year, if available (e.g. 1 Jan 88). Must cite at least the year.

Block 3. Type of Report and Dates Covered. State whether report is interim, final, etc. If applicable, enter inclusive report dates (e.g. 10 Jun 87 - 30 Jun 88).

Block 4. Title and Subtitle. A title is taken from the part of the report that provides the most meaningful and complete information. When a report is prepared in more than one volume, repeat the primary title, add volume number, and include subtitle for the specific volume. On classified documents enter the title classification in parentheses.

Block 5. Funding Numbers. To include contract and grant numbers; may include program element number(s), project number(s), task number(s), and work unit number(s). Use the following labels:

C	- Contract	**PR**	- Project
G	- Grant	**TA**	- Task
PE	- Program Element	**WU**	- Work Unit Accession No.

Block 6. Author(s). Name(s) of person(s) responsible for writing the report, performing the research, or credited with the content of the report. If editor or compiler, this should follow the name(s).

Block 7. Performing Organization Name(s) and Address(es). Self-explanatory.

Block 8. Performing Organization Report Number. Enter the unique alphanumeric report number(s) assigned by the organization performing the report.

Block 9. Sponsoring/Monitoring Agency Names(s) and Address(es). Self-explanatory.

Block 10. Sponsoring/Monitoring Agency. Report Number. (If known)

Block 11. Supplementary Notes. Enter information not included elsewhere such as: Prepared in cooperation with...; Trans. of ..., To be published in .... When a report is revised, include a statement whether the new report supersedes or supplements the older report.

Block 12a. Distribution/Availablity Statement. Denote public availability or limitation. Cite any availability to the public. Enter additional limitations or special markings in all capitals (e.g. NOFORN, REL, ITAR)

DOD	- See DoDD 5230.24, "Distribution Statements on Technical Documents."
DOE	- See authorities
NASA	- See Handbook NHB 2200.2.
NTIS	- Leave blank.

Block 12b. Distribution Code.

DOD	- DOD - Leave blank
DOE	- DOE - Enter DOE distribution categories from the Standard Distribution for Unclassified Scientific and Technical Reports
NASA	- NASA - Leave blank
NTIS	- NTIS - Leave blank.

Block 13. Abstract. Include a brief (Maximum 200 words) factual summary of the most significant information contained in the report.

Block 14. Subject Terms. Keywords or phrases identifying major subjects in the report.

Block 15. Number of Pages. Enter the total number of pages.

Block 16. Price Code. Enter appropriate price code (NTIS only).

Blocks 17. - 19. Security Classifications. Self-explanatory. Enter U.S. Security Classification in accordance with U.S. Security Regulations (i.e., UNCLASSIFIED). If form contains classified information, stamp classification on the top and bottom of the page.

Block 20. Limitation of Abstract. This block must be completed to assign a limitation to the abstract. Enter either UL (unlimited) or SAR (same as report). An entry in this block is necessary if the abstract is to be limited. If blank, the abstract is assumed to be unlimited.

BALLISTIC RANGE FLOWFIELD MEASUREMENTS OF THE HYPERVELOCITY NEAR WAKE OF GENERIC SHAPES AND CORRELATION WITH CFD SIMULATIONS

G. Butler†, D. King* and B. Nguyen*
General Dynamics Convair Division
San Diego, California

G. Abate**
Air Force Armament Laboratory
Eglin Air Force Base, Florida

Abstract

This paper describes analytical and experimental research into the structure and properties of the near wake of generic shapes at supersonic flight conditions. Three axisymmetric model configurations were constructed and tested in the Aeroballistic Research Facility at Eglin Air Force Base, Florida at Mach numbers from 3 to 5 . Laser interferograms were taken of the near wake of the configurations at sea level conditions. Computational interferograms were then developed at identical conditions and were correlated against the experimental data. This correlation will help calibrate high speed CFD codes in this complex flow region.

Background

Recent and ongoing studies have highlighted the renewed interest in vehicles capable of hypersonic operations. These same studies have also shown that currently available ground test facilities are unable to adequately simulate the full range of anticipated flight conditions, and must be supplemented by computational fluid dynamic (CFD) analyses.

CFD simulations,however, cannot be blindly trusted, but must be 'calibrated' against accepted ground or flight test data sets. These data sets must contain some aspect of the critical phenomena of interest to the CFD researcher so that upon successful correlation with the data, an increased understanding and confidence in the particular CFD technique and its applications will be gained.

In addition, CFD solutions for complex hypersonic flowfields are currently too expensive to provide complete vehicle data bases. However, they are essential supplements to ground testing by providing rationale for the extension of ground test data to estimates of vehicle flight characteristics, or by developing accurate estimates of vehicle characteristics directly.

Therefore, hypersonic vehicle development requires a coordinated approach using both ground tests and CFD analyses. Innovative test methods producing the required data at reduced cost are essential to reducing development costs.

The structure and characteristics of the near wake of hypersonic vehicles must be thoroughly understood because of its importance to vehicle performance and its potential ramifications on sensors or other operational considerations. This region is known to contain embedded subsonic recirculations, secondary shocks and extremes in flow pressure, temperature and density (Figure 1)[1]. This presents a very taxing scenario to any experimental or analytical flow resolution technique.

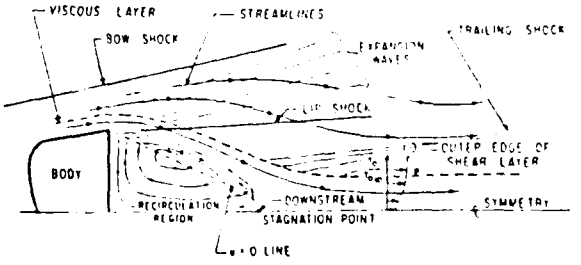

Fig. 1 The near wake of a hypersonic body.

CFD techniques show great promise towards the resolution of such complex flowfields, but as yet must still be calibrated against ground test data to achieve high data confidence levels. The objective of this research,therefore, was to obtain interference-free high Mach number near wake data for the correlation of CFD analyses of the near wake region to support future hypersonic vehicle design efforts.

†Senior Engineer, Member AIAA
*Engineer, Member AIAA
**Aerospace Engineer, Member AIAA

Experimental ground tests for this correlation needed to be devoid of any flow field interference. Wind tunnel testing was deemed inappropriate for this application since the model would be held by a sting of some sort. Therefore, testing needed to be conducted in a free-flight facility capable of obtaining the necessary data.

Experiments

Ground tests were conducted to accomplish two objectives. First and foremost, our objective was the acquisition of data for the correlation of CFD solutions of the hypersonic near wake. Second, testing of additional configurations to qualitatively assess the effects of forebody shaping on the geometry and properties of the hypersonic near wake.

Test Facility

The tests described herein were conducted at the Aeroballistic Research Facility (ARF) located at Eglin AFB, Florida. The ARF is an enclosed, instrumented, concrete structure used to examine the exterior ballistics of various free-flight projectiles. The facility consists of a gun room, control room, model measurements room, blast chamber, and the instrumented range. Figure 2 is a schematic of the ARF and for a complete description of the facility see Reference 2.

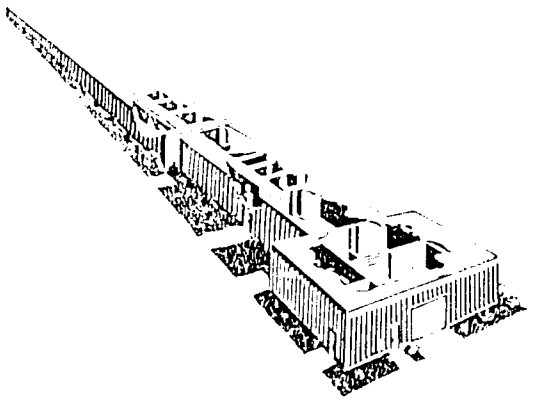

Fig. 2 The Aeroballistic Research Facility.

The ARF is capable of launching models and projectiles to desired velocities by various means. Conventional powder guns, air guns, and a two-stage light-gas gun have been utilized at various times. The two-stage light-gas gun (TGG) was utilized for these tests and is described in References 3 and 4. Successful launch velocities in the Mach 3-6 range are easily attainable using this launcher. Higher velocities to Mach 10 are achievable but launch loads would become a significant factor in the survivability of the package.

Data from the ARF is received in the form of time-position history at discrete locations in the range, direct shadowgrams, laser lighted photographs, and laser interferograms. The shadowgrams and laser photographs give a qualitative assessment of the flight of the model. That is, they would show any model damage or flight anomalies prior to the next test (the laser photography station was not operational for these tests). The time-position history is used for aerodynamic analysis. The data is first fit to linearized equations of motion and subsequently fit using the six-degree-of-freedom equations[5]. The aerodynamic coefficients and stability derivatives can then be extracted from these fits.

Test Description

The one addition to the ARF's instrumentation capability that is not covered in Reference 2 is the installation of an experimental laser Holographic Interferometry Testing (HIT) station. All of the interferograms presented in this paper were obtained using this system. This system is being developed and installed under a contract with the University of Florida. A detailed description of the HIT system and its capabilities will be published in the near future. All that is needed for the purposes of this paper is to point out that the dark lines (see Figs. 3-6), or interference fringes, represent lines of constant density which are integrated along a line perpendicular to the flow. The image is recorded on a holographic plate and must be viewed with a reconstruction laser. A 35mm camera is used to record the interferogram.

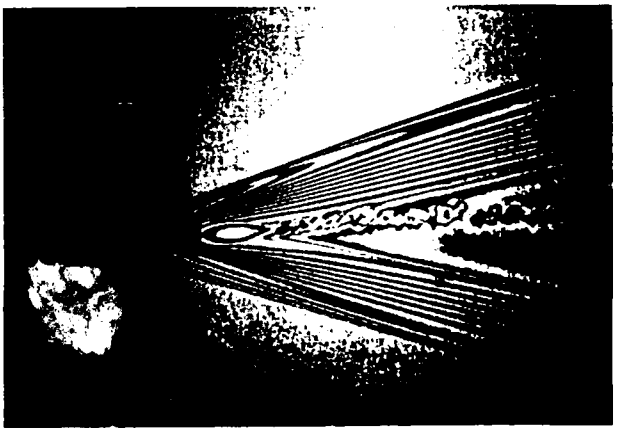

Fig. 3 Infinite fringe interferogram from shot #6.

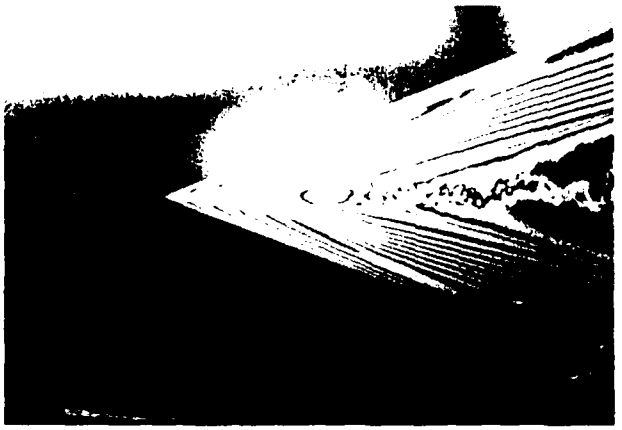

Fig. 4 Infinite fringe interferogram from shot #14.

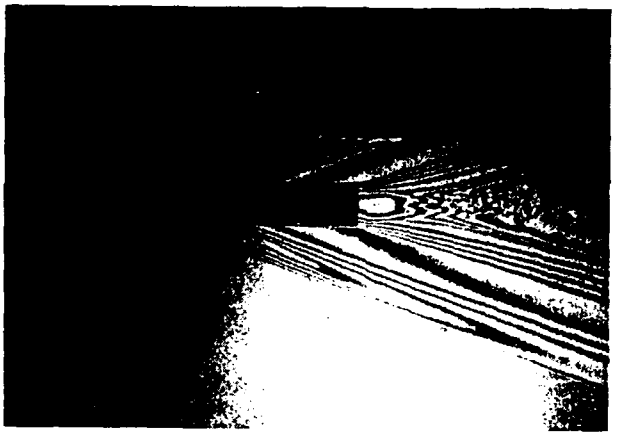

Fig. 5 Infinite fringe interferogram from shot #9.

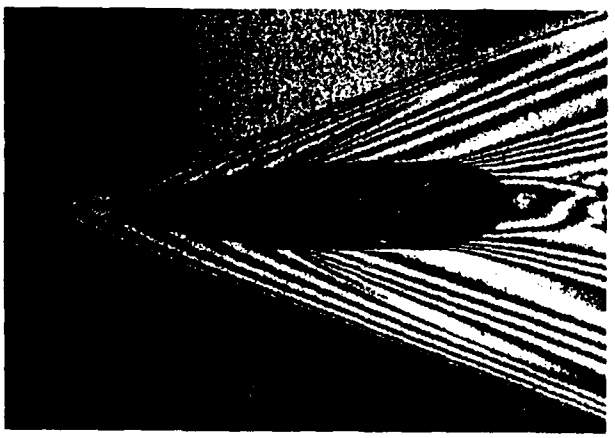

Fig. 6 Infinite fringe interferogram from shot #11.

Although not presented in this paper, the aerodynamics of these projectiles are determined through the use of orthogonal shadowgraph stations. The ARF has 50 shadowgraph stations which record the projectiles position and orientation at specific times. This data is then reduced using data reduction routines specifically written for the range[5]. Usually, the full range is utilized for aerodynamic testing. However, since the primary goal of these tests was to obtain interferograms, the flights were terminated at the one third point of the range.

Originally, the test plan called for these models to be tested in the Mach 5 and above regime. Due to the models heavy nose and hollow base, set back loads in the gun caused catastrophic failure of the model on numerous occasions. Eventually, the cone model was successfully launched near Mach 5 but the cone-cylinder and cone-cylinder-ogive models could only be successfully launched in the Mach 3 to 4 regime. The test plan was then modified to launch the three configurations at one Mach number (Mach 3.5) and plan a series of tests for the cones from Mach 3.5 to 5.5.

Model Design and Construction

Techniques exist for the reduction of axisymmetric interferograms to corresponding density fields and the creation of analytical interferograms from derived axisymmetric density data as a function of position[6]. We have used the latter technique for the preliminary correlation of our CFD solutions, therefore axisymmetric test configurations were required.

Three axisymmetric models of increasing geometric complexity were designed. A basic 10^{o} half angle cone was selected as a baseline because of its simplicity and the wealth of available data on its hypersonic aerodynamic characteristics[7,8,9]. Two additional models, a cone-cylinder (CC) and cone-cylinder-ogive (CCO), were also constructed to study the effects of forebody shaping on the structure and properties of the hypersonic near wake.

The diameter of the models was held constant at 0.75 in. to allow for reasonable launch weights and to insure identical diameter Reynolds numbers. The length of the cone-cylinder and cone-cylinder-ogive models was also fixed at 4.25 in. resulting in identical length Reynolds numbers.

For true axisymmetric flight conditions, the models must be flying without any flow angularity. Therefore, we desired static stability margins, based on diameter, on the order of 10% for each model. Another consideration is flow in the base region. To avoid influencing the near wake, the bases of the models needed to be solid. Therefore, we desired models that were inexpensive, had adequate

stability margins, and would survive the launch loads.

The 10° half-angle cone was 2.125 inches long with a base diameter of 0.75 inches. It was constructed using a brass nose and hollow aluminum aft skirt (see Fig. 7). Both the CC and CCO had a 10° half-angle, 2.125 inch long brass cone hollowed to incorporate a lead insert, followed by a hollow aluminum aft body for an overall model length of 4.25 inches. The 2.125 inches aft body of the CC was 0.75 inches in diameter with a wall thickness of 0.063 inches (Fig. 8). The ogive aft end of the CCO was selected in an attempt to simulate the irrotational flow from the rotational flow at the base of the model, known to occur in axisymmetric wake flows[1,10]. This was done in an attempt to avoid the formation of the recirculation zone which occurs aft of blunt based configurations. At Mach 5 turbulent flight conditions, this line was estimated to terminate at a rearward stagnation point on the centerline 0.9 diameters aft of a basic cone[1,10].

Waldbusser[11,12] has shown the structure and properties of the near wake to be primarily functions of base diameter. Assuming little variation due to forebody shaping, a total ogive length of 0.675 inches was selected to have the ogive terminate at the anticipated rearward stagnation point of the existing 0.75 inch diameter cone-cylinder forebody. The ogive configuration had a major radius of 0.800 inches and a minor radius of 0.125 inches (Fig. 9).

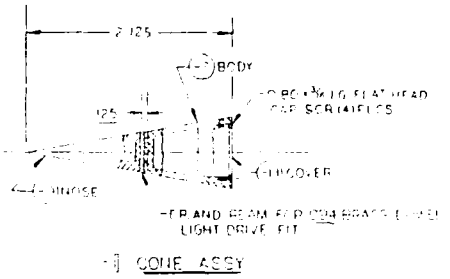

Fig. 7 10° half angle cone model dimensions.

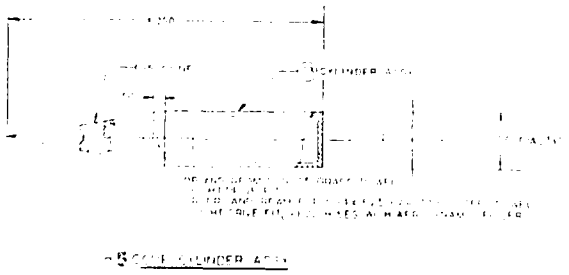

Fig. 8 Cone-cylinder model dimensions.

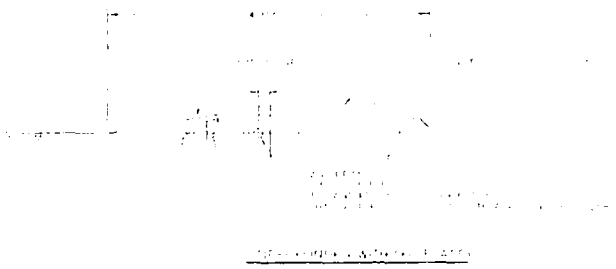

Fig. 9 Cone-cylinder-ogive model dimensions.

Models were encased in a Lexan® sabot and utilized a steel pusher while being launched from the LGG (Fig. 10). During launch, the models were expected to receive axial accelerations on the order of 60,000 g's. A stress analysis was performed at this acceleration level to insure the structural integrity of the pinned and welded plug assembly designed to contain the lead slug.

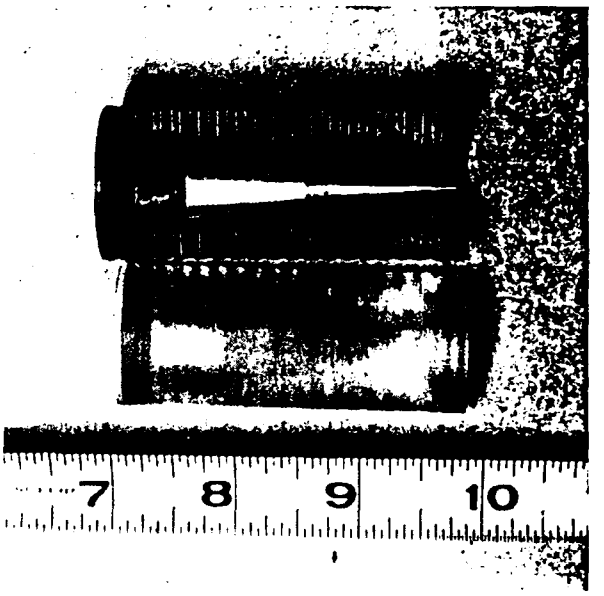

Fig. 10 Cone launch assembly.

Test Results

Table 1 is a summary of the tests performed. Although some of the models were damaged during launch and the HIT station periodically malfunctioned, the test program was successful in that the objectives were met. Interferograms were obtained for each configuration at a relatively constant velocity (Mach 3.1) and high speed cone and cone-cylinder-ogive interferograms were obtained near Mach 4. Unfortunately, interferograms were not obtained for all of the good shots. However, the aerodynamic data recorded [redacted] will be useful in the determination of the aerodynamic coefficients for these models.

Table 1. Summary of Tests Conducted

SHOT #	TYPE	MACH #	COMMENT	INTERGRM
93	C	4.20	GOOD BUT LOW	LATE
06	C	3.87	GOOD	GOOD
07	CC	3.67	MODEL BROKE	
08	CC	3.76	NOSE DAMAGE	
09	CC	3.16	GOOD	GOOD
10	CCO	3.17	GOOD BUT HIGH α	GOOD
11	CCO	3.23	GOOD	GOOD
12	C	3.09	GOOD	MISSED
13	C	3.05	GOOD	MISSED
14	C	3.03	GOOD	GOOD
15	C	4.46	GOOD	MISSED
16	CCO	3.75	GOOD	GOOD

Laser Interferograms

Figure 3 presented an infinite fringe interferogram of the cone configuration taken during shot number 6. The model was at a pitch angle of 5° and yaw angle of 1° as estimated from the post flight data reduction. This is clearly evidenced by the asymmetry evident in the interferogram. The small discontinuity seen in the upper portion of the near wake is thought to be the lip shock, the strength of which may have been increased due to the attitude of the cone.

Figure 4 presented the interferogram resulting from shot number 14. Although the cone has a pitch angle of only -0.75°, post flight data reduction showed that the model was yawed approximately 2°, which cannot be seen from this aspect. The interferogram has good symmetry and clearly illustrates the elliptically shaped contour of extremely low density flow just aft of the model base.

The interferogram resulting from shot number 9 is presented in Figure 5. The model is at a pitch angle of -1° and a yaw angle of -3°. The expansion at the cone-cylinder junction is clearly evident, as are the density contours within the near wake. An initial comparison of Figures 4 and 6 reveals differences in the number and placement of the density contours. This indicates that the near wake structure and properties may be sensitive to forebody shape.

Figure 6 presents the interferogram resulting from shot number 11. Slight asymmetry is evident, again due to the model having a slight pitch angle of approximately 1° and yaw angle of 4.5°. Interestingly, although the ogival aft end did not entirely remove the low density base flow region, the region can be seen to extend less than one diameter from the aft end of the model. Also, two density contours are visible in the near wake region, indicating an increased rate of recovery of density.

CFD Solutions

The CFD solutions were developed using a modified version of the AEDC PARC2D code[13]. The program used a central-difference, implicit time-stepping scheme to solve the full Reynolds averaged Navier-Stokes equation, following the Beam and Warming algorithm[14]. The code was run in the axisymmetric mode.

Assumptions

For the present test cases, the flow was assumed laminar over the cone body. It was hoped that the free-flight test data would show a definite location of transition, however, this was not the case. In addition, the effects of model attitude on the wake flow were assumed small, therefore the solutions were performed at zero angle of attack and sideslip.

Turbulence is evident in the spark photographs at the wake neck (Fig. 11). It is assumed that the flow was laminar in the region before the wake neck. The CFD correlation runs were obtained assuming completely laminar flow, although this is clearly not the case, because of the limited influence of wake turbulence on the density field.

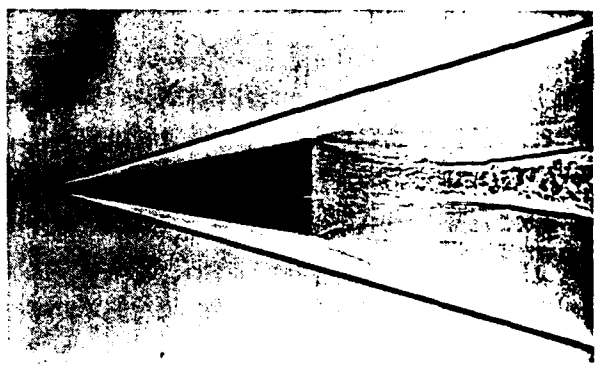

Fig. 11 Spark shadowgram of shot #14.

In flight temperature measurement on the model was not obtained, therefore the wall temperature for the entire body was estimated. Based on the models' temperatures before flight and the short duration of flight prior to reaching the interferogram station (15.5 meters from the end of the gun barrel), an estimate of 80 degrees Fahrenheit was used.

Configuration

The grids used had 155 axial stations and 125 radial stations. The tip of the sharp cone was placed at the 11th axial station, the bases at the 85th axial station. The cone walls were placed at the 57th axial station (meaning that points with axial indices from 1 through

94 and radial indices from 1 through 56 were not used). A typical grid is shown in Fig. 12.

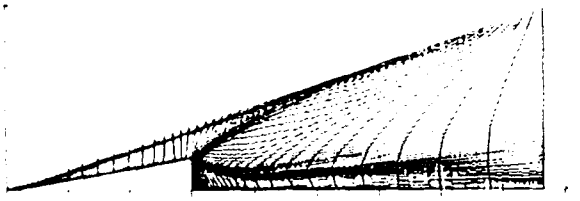

Fig. 12 Typical solution grid for PARC2D.

The solutions generally converged in approximately 1800 iterations. Two to three orders of magnitude reduction in the residual was obtained. In the near wake, adaption to the angle between the acceleration and velocity vectors proved useful to cluster points into the recirculation region as desired.

The CFD solutions showed the general features expected in the flow field. The recompression shock location as well as the location of the wake neck were predicted to occur at approximately 1.0 and 0.8 diameters aft of the cone base for shots 6 and 14 respectively. The test locations were found to be at 1.7 and 1.5 diameters aft.

All spark shadowgrams showed the presence of double lip shocks (very weak shocks emanating from the corner of the cone base, caused by overexpansion and recompression in that vicinity). Both lip shocks were captured in the CFD solutions, but are only evident when viewed with sufficiently fine contour lines. The CFD solution located both lip shocks too close to the centerline (Fig. 13).

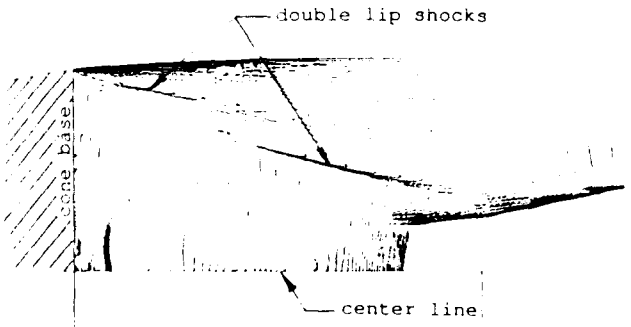

Fig 13 Constant Mach number lines showing lip shocks for CFD simulation of shot #6.

In the case of the cone configuration, the shear layer location correlated well with that shown by the test data. However, the shear layer in the CFD solution appeared wavy (Fig. 14).

In the test data, the near part of the recompression shock was consistently wavy, but the shape of the shear layer was difficult to discern. This waviness may be due in part by the periodic unsteadiness in the real flow and the frequency of large scale turbulence in the wake. These effects were not modelled by the CFD solution.

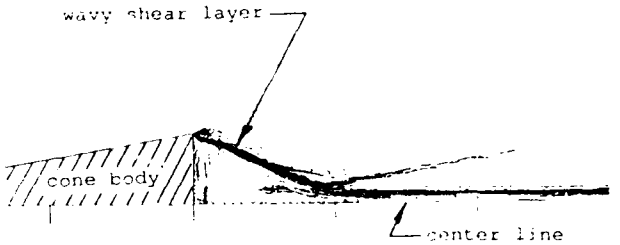

Fig. 14 Constant Mach number line showing details of the CFD shear layer solution.

It is evident from the spark shadowgrams that the frequency of the recompression shock waviness and that of the large scale turbulence are the same and in phase, indicating that the recompression shock waviness is caused by the turbulence. If this is true, then noting that the waviness seemed to have started at the wake necksuggests that the large scale turbulence also started there.

For the cone configuration, a disc-shaped normal shock immediately behind the cone base, centered around the centerline, was captured by the CFD solution, but was not evident from the free-flight test data. In the CFD solution, the flow was accelerated forward from the stagnation point (2 diameters behind the base) to Mach 2.5, and slowed to subsonic speed at 0.1 diameters from the base before turning upward to form the annular recirculation flow.

Other features shown by the CFD solution but unclear in the test data were a primary vortex formed from the shear layer flow and the reversed flow by the centerline. Several secondary vortices also appeared, some turning in the reverse direction (Fig. 15). It is apparent from the numerous vortices in the near wake that flow in that region may be unstable and tend to be unsteady. However, these CFD solution can be applied to understand the mechanisms driving the flow structure in the near wake.

Flowfield Correlations

Initial correlations of the CFD analyses with the test data were performed. These were done qualitatively through the comparison of the ARF test interferograms with simulated

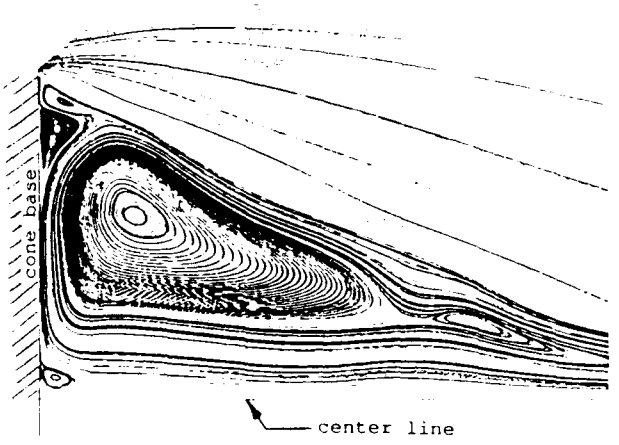

Fig. 15 Near wake countercirculating vortices within the CFD solution.

interferograms developed from the CFD analyses described above.

CFD-Interferogram Interface Code

A computer code for the reduction of CFD derived flowfields to simulated interferograms was obtained from the National Aeronautical and Space Administration's Ames Research Center where it had been used for similar research[8]. The code required some modification to accept the grid structure used for the PARC2D analyses and the particular geometries studied.

The code was applied to develop simulated infinite fringe interferograms from the PARC2D generated density fields. Figure 16 presents the simulated interferogram from the PARC solution corresponding to shot number 6. Similarly, the CFD developed interferogram for shot number 14 is presented in figure 17.

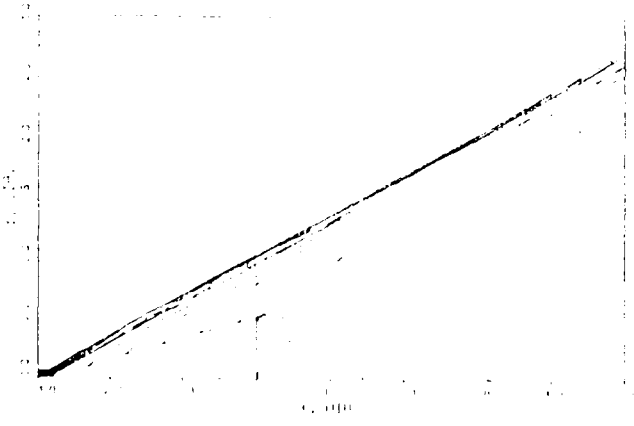

Fig. 16 Analytical interferogram of shot #6.

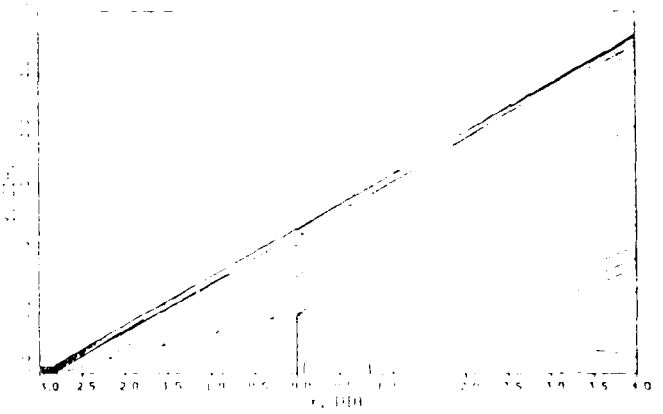

Fig. 17 Analytical interferogram of shot #14.

Correlations

Quantitative correlations were not attempted prior to the publication of this paper. Typically, test interferograms were taken at nonzero model angles of attack, whereas our currently available CFD correlation runs were completed assuming axisymmetric flow. However, we were able to develop qualitative assessments of the accuracy of the CFD solutions.

A comparison of Figures 3 and 16 reveals that the PARC2D solution was able to capture the major features of the flow. A low density contour is seen to extend in the near wake region beyond that evidenced in the test interferogram. This is thought to be attributable to the turbulence within the flow which was not modelled by our PARC solutions, but perhaps may also be caused by unsteadiness in the actual flow.

At the time the interferogram was taken, the model had a positive pitch attitude on the order of 5 degrees. Therefore, six contours are emanating from the cone lower surface while four are seen to emerge from the cone upper surface. The PARC solution for the cone at 0^{o} pitch attitude reveals five contours along the cone upper surface, as would be expected.

An inspection of Figures 4 and 17 reveals significantly better correlations, most likely due to the test interferogram being taken with the model at a significantly lower total angle (2.14^{o}) with respect to the flow. The interferogram has four contours emanating from the cone upper and lower surfaces, with slightly more than $\frac{1}{2}$ diameter spacing between them (moving aft along the cone surface). These contours, and their positions, are accurately predicted by the PARC solution.

Further inspection reveals that the PARC solution was also able to accurately

predict the contours within the near wake region. A total of eight contours are seen to emanate from the base of the cone in both the test and PARC derived interferograms. The innermost contour of the test interferogram is seen to extend approximately 1.25 diameters aft of the cone base. The corresponding PARC contour extends to 0.8 diameters aft. Again, this may be attributable to the exclusion of turbulence modelling.

Conclusions

Interferometric techniques have been shown to be an inexpensive, useful approach towards the correlation of CFD solutions of axisymmetric configurations. This is especially true for tests requiring the non-intrusive acquisition of flowfield data.

In the case of the near wake of axisymmetric configurations, the extremely low densities encountered limit the usefulness of any measurement technique. Interferometry allowed the accurate assessment of the flow properties well into the region of expanded flow and captured sharp gradients (i.e. shocks) accurately.

The PARC2D code was shown to be capable of the accurate analysis of complex, hypersonic flows. Instabilities not encountered in the test data were evident in the PARC solutions, but may be attributed to the periodic unsteadiness of the flow. Additional studies may be required to assess the validity of the aforementioned unsteadiness and secondary recirculation eddies developed in the PARC solution.

For inexpensive correlation of axisymmetric flowfield solutions, models of increased stability should be considered in an attempt to avoid undesirable attitudes during testing. Future tests of this type at velocities greater than Mach 5 should also consider the design and fabrication of solid models. This may be necessary for the models to survive the launch loads at those velocities. The delicate models used for these tests limited attainable velocities. These solid models will probably require the use of exotic materials (e.g. tantalum) to keep the C.G. within limits.

References

1. Martellucci, A., Trucco, H., and Agnone, A., "Measurments of the Near Wake of a Cone at Mach 6," AIAA Journal, Vol. 4, No. 3, 1966.

2. Kittyle, R. L., Packard, J. D., and Winchenbach, G. L., "Description and Capabilities of the Aeroballistic Research Facility," AFATL-TR-87-08, 1987.

3. Swift, H. F., McDonald, J. W., and Chelekis, R. M., "Descriptions and Capabilities of a Two-Stage Light Gas Launcher," Presented at the 35th Meeting of the Aeroballistics Range Association, Meppen FRG, September 1984.

4. Chelekis, R. M., Swift, H. F., and McDonald, J. W., "Descriptions and Capabilities of a High Performance Single Stage Launcher," Presented at the 34th Meeting of the Aeroballistics Range Association, Williamsburg, Va., October 1983.

5. Fischer, M., Hathaway, W. H., "Aeroballistic Research Facility Data Analysis System," AFATL-TR-88-48, 1988.

6. Dunagan, S. E., Brown, J. L., and Miles, J. B., "A Holographic Interferometric Study of an Axisymmetric Shock-Wave/Boundary-Layer Strong Ineraction Flow," AIAA Paper 85-1564, 1985.

7. Murman, E. M., "Experimental Studies of a Laminar Hypersonic Cone Wake," AIAA Journal, Vol 7, No. 9, September 1969.

8. Muntz, E. P., and Softley, E. J., "A Study of Laminar Near Wakes," AIAA Journal, Vol 4, No. 6, June 1966.

9. Lykoudis, P. S., "A Review of Hypersonic Wake Studies," AIAA Journal, Vol 4, No. 4, April 1966.

10. Ragsdale, W. C., and Darling, J. A., "An Experimental Study of the Turbulent Wake Behind a Cone at Mach 5," NOLTR 66-95, 1966.

11. Waldbusser, E., "Geometry of the Near Wake of Pointed and Blunt Hypersonic Cones," AIAA Journal Vol 4, No. 10, October 1966.

12. Waldbusser, E., "Relationship of Laminar Wake Width to Wake Transition Distance," AIAA Journal, Vol 3, No 10, October 1965.

13. Pulliam, T. H., "Euler and Thin Layer Navier-Stokes Codes: Codes ARC2D, ARC3D," Notes for Computational Fluid Dynamics User's Workshop, The University of Tennessee Space Institute, Tullahoma, TN, March 12-16, 1984.

14. Beam, R., and Warming, R. F., "An Implicit Finite-Difference Algorithim for Hyperbolic Systems in Conservation-Law Form," Journal of Computational Physics, Vol 22, No 1, September 1976.